ACS OMEGA

Open Access

http://pubs.acs.org/journal/acsodf

Article

Integrated Couplers of THz Radiation for Helical Slow-Wave Structures

Shiva Hajitabarmarznaki, Shelley A. Scott, Marcos Martinez-Argudo, Divya J. Prakash, Max G. Lagally, Daniel W. van der Weide, and Francesca Cavallo*

Cite This: *ACS Omega* 2024, 9, 35973−35977

Read Online

ACCESS | Metrics & More | Article Recommendations | Supporting Information

ABSTRACT: We have designed an integrated device that couples input and output coaxial horn antennas with a self-assembled helical slow-wave structure cradled in a v-groove on a silicon-on-insulator wafer. These devices will potentially enable the characterization of cold parameters and beam-wave interaction in slow-wave structures on a wafer level, i.e., without having to dice and package individual devices. In addition, such vertically integrated antennas and helical slow-wave structures may form the basis of compact and low-cost traveling-wave tube amplifiers operating at THz frequencies.

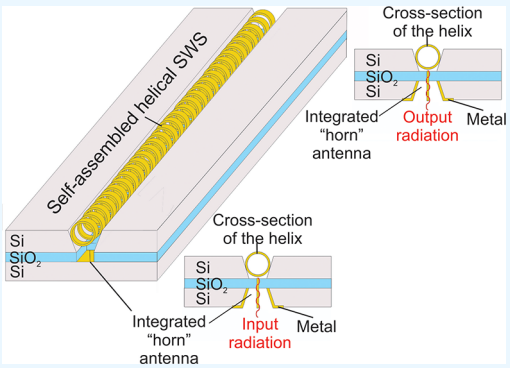

INTRODUCTION

Traveling-wave tube amplifiers (TWTAs) play a crucial role in applications demanding high power, efficiency, bandwidth, and linearity.[1,2] Within a TWTA, a traveling wave confined to a helix-like slow-wave structure (SWS) undergoes amplification through energy exchange with an electron beam. Various applications, including high-speed communications, electronic warfare, and research instrumentation, require scaling TWTAs to operate in the THz range of the electromagnetic spectrum.[3−5] However, the development of TWTAs for THz frequencies presents several challenges,[6,7] including the integration of suitable slow-wave structures (SWSs) with couplers of THz radiation, which is the focus of this work. The characterization and operation of an efficient TWTA require matching input and output structures (couplers) of electromagnetic radiation to the SWS over the desired frequency band. These couplers play a pivotal role in efficiently transmitting radio frequency (RF) signals to and from the SWS. Achieving minimal transmission loss and reducing the reflection of high-frequency signals in TWTAs necessitates a precise match between the SWS and the coupling system. Therefore, the development of structures that facilitate efficient coupling of electromagnetic waves into and out of the helix is vital for TWTAs. Depending on the system requirements, the input and output couplers can be of the coaxial or waveguide type. Coaxial couplers offer wide bandwidths, but the typical average power capability is limited. A waveguide-type coupler can achieve good transmission in a narrow bandwidth with high-power output microwave radiation. Therefore, maximizing the average power capability and the bandwidth of the couplers is an unresolved challenge. Various coupler structures have been reported.[8−12] Srivastava et al.[13] designed input and output couplers for a space helix TWTA. The input coupler consists of a coaxial design, while the output coupler comprises a standard rectangular waveguide (WR-75) and a coaxial coupler to accommodate high output power. Both the input and output couplers exhibited a return loss better than −20 dB across the operating band of 10.9−11.7 GHz. Another study optimized a coaxial coupler as the output for a helix TWTA,[14] achieving an optimized Voltage Standing-Wave Ratio (VSWR) better than 1.5 within the frequency range of 6−18 GHz. In these investigations, the input and output coaxial couplers included components such as windows, impedance transformers, and a transition to a subminiature version A (SMA) connector. It is noteworthy that these previously reported couplers must be assembled with helical SWSs fabricated on a separate substrate. Such a design introduces complexity in implementation and potentially contributes to increased loss. Additionally, none of these efforts outlined above examined structures for operation at THz frequencies, where the cross-sectional dimensions of a TWTA range from a few micrometers to a few tens of micrometers. To our knowledge, the monolithic integration of

Received: June 13, 2024
Revised: July 26, 2024
Accepted: July 30, 2024
Published: August 7, 2024

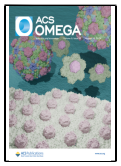

couplers with SWSs for T-waves using scalable processes has not been investigated extensively or demonstrated.

Our previous publications show that self-assembled conductive helices (SACHs) are promising SWSs for millimeter-through-THz TWTAs.[15−19] In this paper, we engineer integrated SACHs with couplers of THz radiation on a single substrate. The proposed design may form the basis of a compact TWTA operating at THz frequencies and intended for use in applications requiring high gain and high output power, such as radar systems, communication satellites, electronic countermeasures, and other warfare systems.[5,6,20,21] Our design includes a SACH fabricated in a v-groove on the front surface of a silicon-on-insulator (SOI) wafer while incorporating input and output coaxial horn antennas on the backside of the same substrate. This geometry will potentially facilitate the characterization of cold parameters and beam-wave interaction in SWSs on a wafer level, thereby eliminating the need to dice and package individual devices for testing. The structures are designed and optimized using CST Microwave Studio (CST-MS). The simulation results predict an insertion loss exceeding −5 dB and a reflection coefficient better than −10 dB across the frequency range from 600 to 700 GHz, with approximately 32% of the incident signal transmitted through the SWS at the desired frequency of 650 GHz. The simulated structures can be fabricated based on established semiconductor industry techniques in combination with the self-assembly of metal ribbons into helical structures. This methodology is feasible on large-area SOI wafers, enabling parallel processing of multiple integrated devices.

RESULTS AND DISCUSSION

Figure 1 illustrates the proposed device for operation within the THz frequency range. The structure consists of three parts:

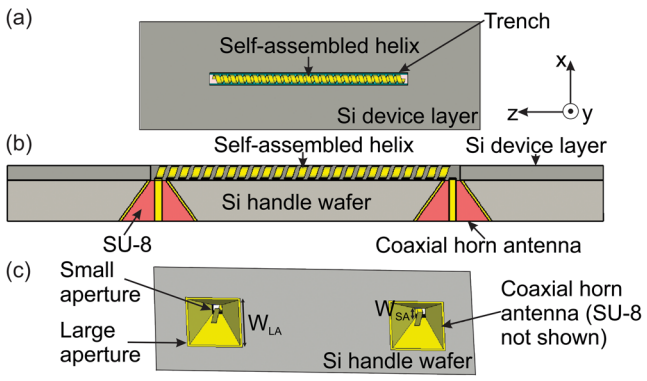

Figure 1. Simulated 3-D structure of coaxial horn antennas integrated with a self-assembled helix. (a) Top view; (b) cross-sectional view; and (c) perspective view from the bottom of the Si handle wafer.

two coaxial horn antennas integrated with a self-assembled helical SWS on a SOI platform. The horn antennas are on the backside of the Si substrate or Si handle wafer. Notably, the horn antennas serve as couplers for the SWS, facilitating injection and collection of THz waves in and out of the helix. The two ends of the helical ribbons extend through the middle of the horn antennas, forming coaxial-like horn structures with a rectangular inner conductor. The cavities of the horn antennas are filled with a dielectric polymer material, i.e., SU8, with a relative permittivity of 3.5 and a loss tangent of 0.0027. The filler improves the stability of the inner conductor of the coaxial horn antennas during further fabrication steps, handling, and operation. The horn geometries can be realized in Si by anisotropic etching of the Si substrate in an alkaline solution, such as KOH.[22,23] This process, which will be detailed later in the manuscript, sets constraints on the thickness of the Si handle wafer, H, and the lateral sizes of the large and the small apertures (W_{LA} and W_{SA}), as specified by eq 1, derived in the Supporting Information,

$$W_{SA} = W_{LA} - 2\cot(54.74^\circ) \times H \quad (1)$$

The device in Figure 1 was modeled and simulated in CST-MS by a frequency-domain solver that uses a tetrahedral mesh. In our simulations, the helix is suspended in free space. Specifically, the helix is not in direct contact with any conductive material above or around it. The purpose of this arrangement is to ensure that the helix operates in an environment free from conductive interference, which could affect the simulation results. Beneath the helix, there is a layer of SiO_2 with a thickness of 1 μm. This SiO_2 layer is positioned at a distance of 4 μm below the helix. We optimized the meshing steps as $D_{x,y,z} = p/8$, where p is the pitch of the helix, to capture accurately the geometry of the helix and minimize simulation time.

The simulated SWS was formed by a metal tape helix with a conductivity of 4.561×10^7 S/m, i.e., the value reported for Au in the CST-MS library. In this study, we assumed a zero RMS surface roughness for the helical tape. The geometrical parameters of the helix, the substrate, and the coaxial horn antennas are listed in Table 1. The cross-sectional areas of the inner conductors, the areas of the small and large apertures of the antennas, the tapering of the horn, and the thickness of the metal coating on the sidewalls of the horns were optimized by a parametric sweep in CST-MS to achieve high coupling efficiency between the SWS and the antennas at 650 GHz. Figure 2 shows the magnitude of the simulated reflection and transmission coefficients versus frequency, denoted as $|S_{11}|$ and

Table 1. Parameters of the Simulated Structure

diameter of the helix, D	pitch of the helix, p	tape width, W	tape thickness, h	length of the helix, L
40 μm	40 μm	24 μm	3.0 μm	1000 μm
thickness: Si handle wafer, H	thickness: buried SiO_2 layer	thickness: Si device layer	area: large aperture of the horn antenna ($W_{LA} \times W_{LA}$)	area: small aperture of the horn antenna ($W_{SA} \times W_{SA}$)
140 μm	1.0 μm	50 μm	250 × 250 μm^2	50 × 50 μm^2

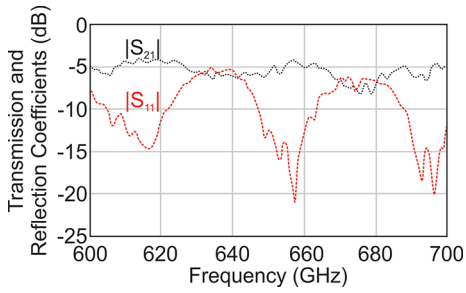

Figure 2. Magnitude of the simulated reflection ($|S_{11}|$) and transmission ($|S_{21}|$) coefficients of the device. The incident and reflected powers are measured at port 1. The transmitted power is measured at port 2.

https://doi.org/10.1021/acsomega.4c05562
ACS Omega 2024, 9, 35973−35977

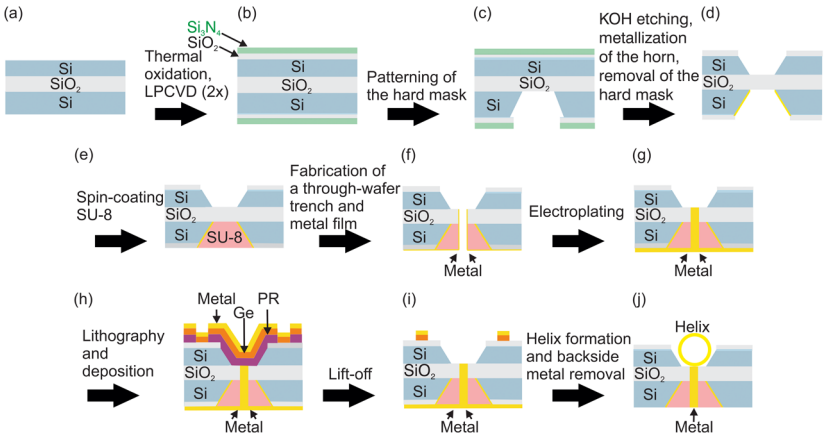

Figure 3. Cross-sectional schematic diagrams of the device at selected stages of the fabrication process. All dimensions were determined from simulations. (a) SOI with layer thicknesses (top to bottom) 5 μm Si, 1 μm oxide, 140 μm Si handle. (b) Etch mask formation. (c) Mask patterning. (d) After KOH etching, the bottom antennas are metallized. (e) SU8 is used to fill the back cavity. (f) A through-hole is formed and coated with an electroplatable metal, e.g., Au. (g) A metal strip is formed by electrodeposition, connecting the top and bottom etched structures. (h) The contact pads and helix arm trenches are defined with photolithography, followed by Ge and then Au deposition. (i) Lift-off removes the excess Ge/metal. (j) A helical SWS is formed by selectively etching the Ge layer. Thicknesses and lateral dimensions are not to scale.

$|S_{21}|$, respectively. The simulation calculated an insertion loss exceeding −5 dB and a reflection coefficient better than −10 dB across most of the frequency range from 600 to 700 GHz. Approximately 32% of the incident signal is transmitted through the slow-wave structure (SWS) at the target frequency of 650 GHz, while only ∼8% of the incident signal is reflected. These results validate the efficacy of the coaxial horn antennas in coupling the THz radiation in and out of the helical SWS. We speculate that insertion losses are due to the radiation of the electromagnetic energy into free space and the dissipation of electromagnetic power in the metal helix. Additional studies are required to confirm our hypothesis and will be published elsewhere, as the focus of this work is the integration of efficient couplers of THz radiation with the helical SWS.

The device in Figure 1 can be fabricated via a combined top-down/bottom-up process on a commercially available silicon-on-insulator (SOI) wafer (see Figure 3). In this process, the bulk (or handle) Si substrate in the SOI is thinned via grinding from the backside to the handle wafer thickness determined from simulations (Figure 3a). The front and the back side of the SOI wafers are then thermally oxidized. Subsequently, a silicon nitride film is deposited onto the thermally grown SiO_2 to form a bilayer hard mask (Figure 3b). Square openings are patterned in the oxide/nitride bilayers of the back side of the Si handle wafer using conventional top-down patterning techniques (Figure 3c). The cross-sectional areas of these windows match the size of the optimal large aperture of the coaxial horn antennas, i.e., 250 × 250 μm^2 (Figure 3c). A rectangular window is also fabricated in the front-Si hard mask. The unprotected Si handle wafer and Si device layer are anisotropically wet etched in potassium hydroxide (KOH) to define the shape of the coaxial horn antennas and the groove that will cradle the SWS after its fabrication. The Si_3N_4 mask is removed in an H_2PO_4 solution, and the trenches on the back side of the SOI wafer are metalized to a film thickness of 10 μm with a combination of thin-film deposition and electroplating (Figure 3d). Note that the bottom of the pyramid is masked (using either a direct mask or photoresist and lift-off) to prevent metal deposition in the region that will eventually be in contact with the central metal strip. The backside cavity is filled with a dielectric polymer (i.e., SU8) via spinning the polymer and photolithographic masking and etching to remove the remaining material surrounding the cavity (Figure 3e). A 3 μm × 24 μm through-hole is formed between the backside and frontside etched regions using photolithography and etching of the SU8. The SU8 serves as a mask for Cl- and F-based reactive ion etching of the oxide layer. Metal is introduced into the trench via physical vapor deposition to generate a seed layer (Figure 3f) for electroplating, forming the Au strip (Figure 3g). The helix is fabricated by the release of patterned metal strips on the front side of the SOI wafer (Figure 3h). For this purpose, a sacrificial Ge layer is deposited over patterned photoresist (PR), followed by the deposition of a stressed metal layer. Lift-off removes the excess Ge and metal, leaving behind a pattern that typically includes large pads or a wide frame (Figure 3i). The helical SWS is fabricated on the front side of the wafer, according to the methods already disclosed in ref 1. Here, the Ge is selectively etched in either hot water or H_2O_2, causing the metal strip to curl and twist, forming a helix (Figure 3j).

Figure 4 shows a top-view schematic diagram of a proposed device before and after the release of a metal strip anchored to large-area pads. Metal strips on a Ge sacrificial layer can be fabricated by photolithography, physical metal deposition, and lift-off. During deposition, a residual stress gradient builds up across the thickness of the metal film. The two narrow metal

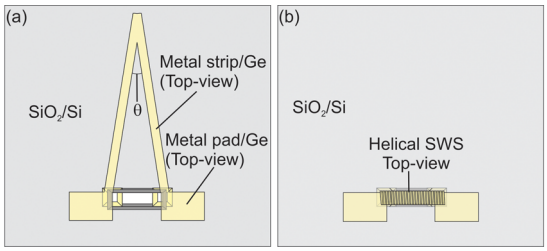

Figure 4. Schematic diagrams showing the structure and layers of the helical SWS coupled to an input and an output antenna. (a) This view shows the arms and contact pads that were defined in Figure 3h,i in relation to the top-side trench and the input and output antennas. (b) After the Ge is selectively etched, the Au arm strips relieve stress by curling into a helix.

https://doi.org/10.1021/acsomega.4c05562
ACS Omega 2024, 9, 35973−35977

strips in Figure 4a form an angle θ and are connected to large-area islands or pads. The metal strips release and self-assemble into a helix as the Ge sacrificial layer is selectively etched. Self-assembly results from the relaxation of the residual stress in the metal, which drives the film to bend out of the plane of the substrate surface. The fabricated helix cradles into the trench fabricated on the front side of the SOI wafer with its two tethered ends aligned with the coaxial horn antennas on the Si handle wafer (see Figure 4b). The diameter of the helix is controlled by the stiffness of the metal strips and the stress profile across their thickness. The pitch of the helix for a given diameter is determined by the angle, α, between the two strips. Additional details on the fabrication of conductive helices by guided self-assembly of metal strips or ribbons are reported in our previous works.[13−17]

CONCLUSIONS

We have reported the design of a helical slow-wave structure with integrated couplers of THz radiation. The device geometry is optimized to operate at 650 GHz via numerical simulations, but the structure can be scaled for operation at different millimeter-through-THz frequencies. The novelty of the architecture is in the use of coaxial horn antennas as couplers and their integration with a self-assembled helical slow-wave structure (SWS) on the same Si wafer. This device eliminates the need for assembly of couplers and SWSs fabricated on different supports, which increases the loss and reduces the reliability and stability of operation over time. Simulation results provided an insertion loss exceeding −5 dB and a reflection coefficient better than −10 dB between 600 to 700 GHz, with approximately 32% of the incident signal transmitted through the SWS at the target frequency of 650 GHz. In addition to demonstrating transmission of the THz waves via a computational study, we have laid out a path to the fabrication of the devices based on widely established top-down techniques in the semiconductor industry in combination with the self-assembly of metal ribbons into helical structures. The approach is realizable on a large-area Si wafer for parallel processing of multiple integrated devices.

ASSOCIATED CONTENT

Supporting Information

The Supporting Information is available free of charge at https://pubs.acs.org/doi/10.1021/acsomega.4c05562.

Text and figure deriving eq 1, i.e., the relationship between the small and the large apertures of the coaxial horn antennas (PDF)

AUTHOR INFORMATION

Corresponding Author

Francesca Cavallo − *Center for High Technology Materials, University of New Mexico, Albuquerque, New Mexico 87106, United States; Department of Electrical and Computer Engineering, University of New Mexico, Albuquerque, New Mexico 87131, United States;* orcid.org/0000-0003-2498-3649; Email: fcavallo@unm.edu

Authors

Shiva Hajitabarmarznaki − *Department of Electrical and Computer Engineering, University of Wisconsin-Madison, Madison, Wisconsin 53706, United States*

Shelley A. Scott − *Department of Materials Science and Engineering, University of Wisconsin-Madison, Madison, Wisconsin 53706, United States;* orcid.org/0000-0002-1263-011X

Marcos Martinez-Argudo − *Department of Electrical and Computer Engineering, University of Wisconsin-Madison, Madison, Wisconsin 53706, United States*

Divya J. Prakash − *Center for High Technology Materials, University of New Mexico, Albuquerque, New Mexico 87106, United States*

Max G. Lagally − *Department of Materials Science and Engineering, University of Wisconsin-Madison, Madison, Wisconsin 53706, United States*

Daniel W. van der Weide − *Department of Electrical and Computer Engineering, University of Wisconsin-Madison, Madison, Wisconsin 53706, United States*

Complete contact information is available at: https://pubs.acs.org/10.1021/acsomega.4c05562

Notes

The authors declare no competing financial interest.

ACKNOWLEDGMENTS

This work was funded by the U.S. Air Force Office of Scientific Research under award No. FA9550-22-1-0301.

REFERENCES

(1) Paoloni, C. Sub-THz Wireless Transport Layer for Ubiquitous High Data Rate. *IEEE Communications Magazine* **2021**, *59* (5), 102−107.

(2) Chong, C. K.; Cordrey, D. A.; Dawson, R. C.; Forster, J. W.; Layman, D. A.; Ramay, M. L.; Stolz, R. J.; Washington, C. D., High Power Millimeter Wave Helix TWT Programs at L-3 ETI. *2013 IEEE 14th International Vacuum Electronics Conference (IVEC)*; IEEE, 2013.

(3) Paoloni, C.; Di Carlo, A.; Bouamrane, F.; Bouvet, T.; Durand, A. J.; Kotiranta, M.; Krozer, V.; Megtert, S.; Mineo, M.; Zhurbenko, V. Design and Realization Aspects of 1-THz Cascade Backward Wave Amplifier Based on Double Corrugated Waveguide. *IEEE Trans. Electron Devices* **2013**, *60* (3), 1236−1243.

(4) Zuboraj, M.; Apaydin, N.; Sertel, K.; Volakis, J. L. Half-Ring Helical Structure for Traveling Wave Tube Amplifiers. *IEEE Transactions on Plasma Science* **2014**, *42* (11), 3465−3470.

(5) Kory, C.; Ives, L.; Read, M.; Phillips, P.; Booske, J.; Bhattacharjee, S.; Welter, J.; Genack, M.; Jiang, H.; van der Weide, D. W.; Limbach, S.; Borchard, P. In Novel TWT Interaction Circuits for High Frequency Applications, *Fifth IEEE International Vacuum Electronics Conference (IEEE Cat. No.04EX786), 27−29 April 2004*; IEEE, 2004; 51−52.

(6) Booske, J. H.; Dobbs, R. J.; Joye, C. D.; Kory, C. L.; Neil, G. R.; Park, G. S.; Park, J.; Temkin, R. J. Vacuum Electronic High Power Terahertz Sources. *IEEE Transactions on Terahertz Science and Technology* **2011**, *1* (1), 54−75.

(7) Booske, J. H. Plasma Physics and Related Challenges of Millimeter-Wave-to-Terahertz and High Power Microwave Generation. *Phys. Plasmas* **2008**, *15* (5), No. 055502.

(8) Wu, G. X.; Yin, H. R.; Xu, Z.; Yang, R. C.; Xia, L.; Li, Q.; Yue, L. N.; Xu, J.; Zhao, G. Q.; Park, G. S.; Wei, Y. Y. Design and Experimental Measurement of Input and Output Couplers for a 6−18-GHz High-Power Helix Traveling Wave Tube Amplifier. *IEEE Trans. Electron Devices* **2020**, *67* (4), 1826−1831.

(9) Chen, K.; Yue, L. N.; Lv, S. Z.; He, J.; Wang, W. X.; Wei, Y. Y., Design of a Coaxial Coupler for an E-band Helix Traveling-Wave Tube. *IVEC 2021:2021 22nd International Vacuum Electronics Conference*, 2021.

(10) Alaria, M. K.; Sinha, A. K.; Bera, A.; Srivastava, V. Design of Coaxial Couplers for High Efficiency Helix TWT. *International Journal of Infrared and Millimeter Waves* **2008**, *29* (12), 1083−1090.
(11) Wang, J. X.; Liu, G.; Shu, G. X.; Yang, L. Y.; Luo, Y. Design and Microwave Measurement of a Broadband Compact Power Coupler for Sheet Beam Traveling Wave Tubes. *IEEE Trans. Electron Devices* **2016**, *63* (2), 814−818.
(12) Letizia, R.; Mineo, M.; Paoloni, C. Photonic Crystal-Coupler for Sheet Beam THz Vacuum Electron Tubes. *IEEE Electron Device Lett.* **2016**, *37* (9), 1227−1230.
(13) Srivastava, V.; Srivastava, A.; Singh, V. V. P.; Chandan, S. In Design of Input and Output Couplers for Ku-band 140 W Space TWT, *4th IEEE International Conference on Vacuum Electronics, 2003, 28−30 May 2003*; IEEE, 2003; 165−166.
(14) Ghosh, T. K.; Carter, R. G.; Challis, A. J.; Rushbrook, K. G.; Bowler, D. Optimization of Coaxial Couplers. *IEEE Trans. Electron Devices* **2007**, *54* (7), 1753−1759.
(15) Prakash, D. J.; Dwyer, M. M.; Argudo, M. M.; Debasu, M. L.; Dibaji, H.; Lagally, M. G.; van der Weide, D. W.; Cavallo, F. Self-Winding Helices as Slow-Wave Structures for Sub-Millimeter Traveling-Wave Tubes. *ACS Nano* **2021**, *15* (1), 1229−1239.
(16) Argudo, M. M.; Hajitabarmarznaki, S.; Prakash, D. J.; Dwyer, M. M.; Lagally, M. G.; van der Weide, D. W.; Cavallo, F. Amplification of THz waves by Beam-Wave Interaction in Self-Assembled Helical Slow-Wave Structures with Single and Double chirality. *AIP Adv.* **2022**, *12* (8), No. 085121.
(17) Prakash, D. J.; Martinez-Argudo, M.; Hajitabarmarznaki, S.; Lagally, M. G.; van der Weide, D. W.; Cavallo, F. In Design and Fabrication of Devices for Characterization of Cold Parameters in Self-Assembled Metal Helices, *2022 23rd International Vacuum Electronics Conference (IVEC), 25−29 April 2022*; 2022; 182−183.
(18) Prakash, D. J.; Vijayamohanan, J.; Heilman, G. D.; Chaudhary, A.; Lagally, M. G.; van der Weide, D. W.; Christodoulou, C.; Cavallo, F. In Characterization of Self-Assembled Helical Slow-Wave Structures for Millimeter-Wave Traveling-Wave Tube Amplifiers, *2022 15th UK-Europe-China Workshop on Millimetre-Waves and Terahertz Technologies (UCMMT), 17−18 Oct. 2022*; IEEE, 2022; 1−3.
(19) Prakash, D. J.; Argudo, M. M.; van der Weide, D. W.; Cavallo, F. In Design and Fabrication of Self-Assembled Metal Helices for Millimeter-through- THz Traveling Wave Tube Amplifiers, *2021 14th UK-Europe-China Workshop on Millimetre-Waves and Terahertz Technologies (UCMMT), 13−15 Sept. 2021*; IEEE, 2021; 1−3.
(20) Booske, J. H.; Kory, C. L.; Gallagher, D.; Heinen, V.; Kreischer, K.; van der Weide, D. W.; Limbach, S.; Gustafson, P.; Lee, W. J.; Gallagher, S.; Jain, K. In Terahertz-Regime, Micro-VEDs: Evaluation of Micromachined TWT Conceptual Designs, *IEEE Conference Record - Abstracts. PPPS-2001 Pulsed Power Plasma Science 2001. 28th IEEE International Conference on Plasma Science and 13th IEEE International Pulsed Power Conference (Cat. No.01CH37, 17−22 June 2001*; IEEE, 2001; 161.
(21) Dayton, J. A.; Kory, C. L.; Mearini, G. T.; Malta, D.; Lueck, M.; Gilchrist, K. In Applying Microfabrication to Helical Vacuum Electron Devices for THz Applications, *2009 IEEE International Vacuum Electronics Conference, 28−30 April 2009*; IEEE, 2009; 41−44.
(22) Seidel, H.; Csepregi, L.; Heuberger, A.; Baumgärtel, H. Anisotropic Etching of Crystalline Silicon in Alkaline Solutions: I. Orientation Dependence and Behavior of Passivation Layers. *J. Electrochem. Soc.* **1990**, *137* (11), 3612.
(23) Seidel, H.; Csepregi, L.; Heuberger, A.; Baumgärtel, H. Anisotropic Etching of Crystalline Silicon in Alkaline Solutions: II. Influence of Dopants. *J. Electrochem. Soc.* **1990**, *137* (11), 3626.

https://doi.org/10.1021/acsomega.4c05562
ACS Omega 2024, 9, 35973−35977